

Bianca N. I. Eskelson¹, Department of Forest Engineering, Resources and Management, Oregon State University, Corvallis, Oregon 97331

Paul D. Anderson, Pacific Northwest Research Station, USDA Forest Service, Corvallis, Oregon 97331

and

Hailemariam Temesgen, Department of Forest Engineering, Resources and Management, Oregon State University, Corvallis, Oregon 97331

Modeling Relative Humidity in Headwater Forests Using Correlation with Air Temperature

Abstract

Microclimate variables such as air temperature and relative humidity influence habitat conditions and ecological processes in riparian forests. The increased relative humidity levels within riparian areas are essential for many plant and wildlife species. Information about relative humidity patterns within riparian areas and adjacent uplands are necessary for the prescription of effective buffer widths. Relative humidity monitoring is more expensive than temperature monitoring due to greater sensor costs, and it is primarily conducted for research purposes. To make relative humidity monitoring in riparian areas more cost effective, we explored modeling relative humidity as a function of air temperature and other covariates using linear fixed and linear mixed effects models applied to two case studies. Localizing predictions for stream reaches using a linear mixed effects model or a linear fixed effects model with correction factor improved model predictions, especially when large variability among stream reaches was present. A minimum of three to five relative humidity measurements per stream reach seem sufficient to estimate the random stream reach effect or correction factor for the linear mixed and linear fixed effects models, respectively. Including covariates that describe distance to stream and canopy cover in addition to air temperature improved model performance. Although further model refinement is probably needed to allow detection of small changes in relative humidity associated with changes in stand structure from partial overstory removal, the models developed provide a means towards decreasing the costs of monitoring microclimates of importance to riparian area function.

Keywords: riparian microclimate; Pacific Northwest; linear mixed effects model; localized prediction; subsampling

Introduction

Riparian areas within forest landscapes are distinct in supporting relatively high levels of biodiversity (Olson et al. 2007). The combination of hydrologic and fluvial processes, disturbance regimes, and the exchange of energy and matter among terrestrial and aquatic systems (Gomi et al. 2002, Nakano and Murakami 2001) contributes to diverse habitats and complex trophic structures within riparian areas. For seasonally dry temperate forests, microclimates are often distinctly different between riparian areas and the adjoining terrestrial forest; riparian areas with greater soil moisture or open water surfaces tend to be cooler and more humid than surrounding uplands (Rykken et al. 2007,

Brooks and Kyker-Snowman 2009). Influences of clear cutting and partial overstory removal on stream and riparian microclimate has received much attention, and the interest has expanded upstream to encompass the extensive but small and often non-fish bearing perennial or ephemeral headwaters streams (Chen et al. 1999, Brooks and Kyker-Snowman 2009, Anderson et al. 2007).

Headwater plant and animal communities can demonstrate a high degree of spatial structuring within a relatively compressed area (Pabst and Spies 1998, Sheridan and Olson 2003, Sheridan and Spies 2005, Olson and Weaver 2007). This spatial structuring of communities is likely associated with gradients in microclimate, particularly air temperature and relative humidity, as a function of lateral distance from stream, which for complex, steep topography implies gradients with

¹Author to whom correspondence should be addressed.
Email: bianca.eskelson@oregonstate.edu

height above stream (Pabst and Spies 1998, Sheridan and Spies 2005).

Monitoring of stream channel and riparian area relative humidity has been conducted primarily as a research activity to characterize habitat associations and ecosystem processes, which may partly be due to the high costs of sensors that measure relative humidity. To use relative humidity for forest management or regulatory purposes, effective and efficient means for characterizing and monitoring relative humidity in these biologically diverse riparian settings need to be identified.

Strong negative correlations between relative humidity and air temperature are often observed in forest ecosystems (Chen et al. 1999). Strength of association arises in part from the physical characteristics of water vapor as a component of air (Jones 1992) and in part from the biophysical process of transpiration (Landsberg 1986). Given relative humidity and air temperature are strongly correlated, the question arises whether this strong relationship can be exploited in modeling relative humidity for locations for which measured air temperature information are available. If relative humidity can successfully be modeled, the number of relative humidity sensors within a stream reach could be reduced, thus reducing the cost of relative humidity monitoring. To our knowledge, no work has been done to model relative humidity as a function of air temperature and other covariates with the purpose of reducing the costs of relative humidity sampling. Our objectives were to use data from two case studies to:

- a) provide an overview on summer correlations between mean daily minimum relative humidity (RH_{\min}) and mean daily maximum air temperature (Ta_{\max}) across stream reaches and watersheds;
- b) assess the abilities of linear fixed and linear mixed effects models to predict RH_{\min} as a function of Ta_{\max} and other covariates; and
- c) compare accuracy and precision of RH_{\min} predictions under varying sample size, and discuss the impact on sampling and monitoring costs.

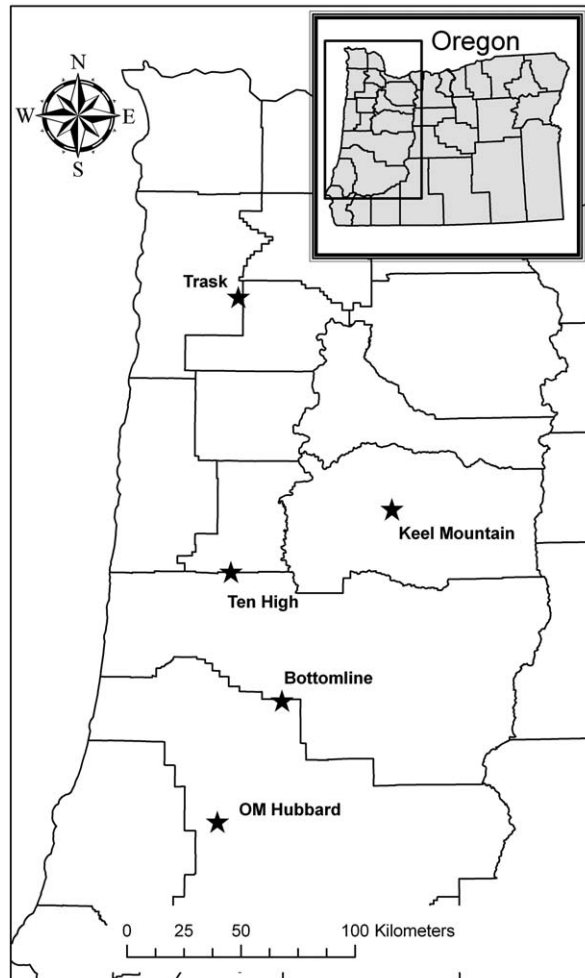


Figure 1. Map showing the location of the Trask watershed and the Density Management Study sites.

Methods

Our study uses microclimate data collected in eight stream reaches of the Trask watershed in the Coast Range in northwest Oregon (Trask Study Plan 2008) and eight stream reaches that are part of the Density Management Study (DMS; see Cissel et al. 2006) in the central Oregon Coast Range and western Cascade Range (Figure 1).

Trask Data

The Trask watershed in northwest Oregon is part of a paired watershed study to evaluate the effects of forest harvest (Trask Study Plan 2008). During

the summer of 2009, microclimate sensors (Hygrochron i Button, model DS1923, Maxim Integrated Products, Inc., San Jose, CA) were deployed at eight stream reaches that are part of the paired watershed study. Stream reaches were located along second order headwater streams and at the downstream portion of the watersheds or basins that were to be harvested or serve as reference basins. The stream reaches were selected to have upstream areas of approximately 35-55 ha. At every stream reach, six transects were located perpendicular to the stream (three on each side). The location of the first transect was randomly selected and the remaining transects were then installed 40 to 60 m upstream of the previous transect, alternating on stream sides. Two microclimate sensors were deployed on each of the six transects 12 m apart, with the first sensor having a random distance between 4 m and 8 m to the stream. The sensors were rotated among the eight stream reaches, and twelve sensors were deployed at each stream reach for approximately four consecutive weeks or longer (Table 1). Air temperature and relative humidity were measured at 1 m above ground every hour. Mean daily estimates of the minimum relative humidity (RH_{\min}) and the maximum air temperature (Ta_{\max}) were computed for each sensor for the duration of the sensor deployment (Table

1). The Trask data consist of $n = 95$ RH_{\min} and Ta_{\max} observations, because one sensor in stream reach RK2 failed during deployment.

Density Management Study Data

The DMS is an operational-scale multidisciplinary evaluation of alternative thinning regimes applied to 35-65 year-old managed Douglas-fir (*Pseudotsuga menziesii* [Mirb.] Franco) stands in headwater forests of western Oregon. Study treatments are comprised of three thinning intensities and unthinned references. Embedded within overstory treatment units are small headwater streams buffered to an array of widths (Cissel et al. 2006). In our study we report on microclimate data collected from a random sample of eight stream reaches distributed among three DMS study locations (Table 1). Reaches were defined as unbranched stream segments of at least 100-m length between nodes in the stream network and contained entirely within the boundaries of a single upland overstory treatment unit. Sampled stream reach buffers ranged from 25-145 m width, side slopes ranged from 18-51% and bankfull stream width ranged from approximately 0.3 m to 2.6 m.

TABLE 1. Sensor deployment dates and number of sensors (n_i) in the eight Trask and DMS stream reaches.

Trask Stream Reach	n_i	Sensor Deployment in 2009	DMS Stream Reach	n_i	Sensor Deployment in 2006
Gus Creek 1 (GS1)	12	7/10 – 8/6	Bottom Line, reach 13 (BL13)	64	9/5 – 9/11
Gus Creek 3 (GS3)	12	7/7 – 8/13	Keel Mountain, reach 17 (KM17)	65	8/29 – 8/31
Pothole Creek 2 (PH2)	12	7/25 – 8/21	Keel Mountain, reach 18 (KM18)	61	7/19 – 7/24
Pothole Creek 3 (PH3)	12	7/28 – 8/27	Keel Mountain, reach 19 (KM19)	50	8/15 – 8/23
Pothole Creek 4 (PH4)	12	8/19 – 9/30	Keel Mountain, reach 21 (KM21)	65	8/24 – 8/29
Rock Creek 2 (RK2)	11	8/22 – 9/30	OM Hubbard, reach 36 (OM36)	65	9/12 – 9/19
Rock Creek 3 (RK3)	12	8/28 – 9/30	Ten High, reach 46 (TH46)	62	8/8 – 8/16
Upper Main 3 (UM3)	12	8/7 – 9/30	Ten High, reach 75 (TH75)	64	8/1 – 8/7

A 72 m x 72 m (0.518 ha) sampling plot, centered on the central axis (center line, CL) of the channel was established at a random longitudinal position along each of eight stream reaches. Micro-climate (air temperature and relative humidity) was monitored along 72-m transects that traversed the stream perpendicular to the CL. For each stream reach two sets of transects were monitored: 1) two transects located at 32 and 68 m along the CL with sample points spaced at 3 m horizontal distance intervals; and 2) two transects randomly located within 0-32 m and 32-64 m intervals along the CL with sample points distributed at 10 m horizontal distance intervals along each transect (see Eskelson et al. 2011). In addition to horizontal distance, the slope distance, and height above stream (HAS [elevation above the stream surface]) was determined for each sample point. Canopy transmittance of solar energy was estimated using light detection within a vertically-oriented hemispherical field of view above each sample point. Measurements of diffuse, non-intercepted radiation (DIFN) at 1 m height above ground, relative to the potential received above the canopy for the geographic location, were made using a plant canopy analyzer (model LAI-2000, LI-COR Biosciences, Lincoln, NE).

Air temperature and relative humidity data were collected using integrated 3-channel data loggers (models GPSE 101 203 and GPSE 301 203, A.R. Harris Ltd., Christchurch, New Zealand). The air temperature/relative humidity sensors were positioned 1 m above ground with an inverted 1-liter ventilated plastic cup providing shade. Data were logged at 20 minute intervals. Sensors were deployed to the eight reaches at different times in mid- to late-summer for 3-8 consecutive days (Table 1). For analysis, data from individual sensors were initially reduced to hourly values and truncated to the warmest 3-day period sampled for each reach. Data were then reduced to 3-day averages of daily maximum hourly air temperature ($T_{a_{max}}$) and daily minimum hourly relative humidity (RH_{min}), which were used in assessments of temperature-relative humidity correlation and for modeling relative humidity as a function of air temperature. Due to data logger failures, 50 to 65 sample points per stream reach were independently

monitored, resulting in $n = 495$ observations for the DMS data.

Models

Three modeling strategies were used to predict RH_{min} as a function of $T_{a_{max}}$ and other covariates. The first modeling strategy was a linear fixed effects model (LFEM), for the second strategy a stream reach correction factor was calculated and applied to the predicted values from LFEM (LFEMcf), and the third strategy was a linear mixed effects model (LMEM) with a random intercept. All models were fit with the R software (R Development Core Team 2011) using the functions `gls()` and `lme()`.

Linear Fixed Effects Model—The linear fixed effects model (LFEM) assumes independent observations within and among stream reaches. For the Trask data, $T_{a_{max}}$ was the only covariate in the model, whereas HAS and DIFN were additional covariates for the DMS model. Because of the small number of observations available for each stream reach in the Trask, additional covariates were not included in the models for the Trask. The nested data structure violates the assumption of independence of the LFEM model; it is included in our analysis to show the implications of decisions made using the model when the assumption of independence is violated. A power variance function accounted for heteroscedasticity. The residuals showed weak departure from normality. For the Trask the residuals were slightly skewed to the right and for the DMS they had heavy tails. The impact of the weak departure from normality on the model was considered negligible. For model details see Appendix A1.

Linear Fixed Effects Model with Correction Factor—If a subsample (n_m) of RH_{min} values is known for a new stream reach m , the subsampled information can be used to localize RH_{min} predictions for the new stream reach with a correction factor k_m^* (Strategy 4 in Temesgen et al. 2008). This model will be referred to as LFEMcf (see details in Appendix A2). LFEMcf violates the assumption of independence when the model is fit and tries to account for the nested data structure in the prediction process.

Linear Mixed Effects Model with Random Intercept—The linear mixed effects model (LMEM) includes a random stream reach effect b_i which allows the intercept to vary by stream reach, thus localizing RH_{\min} predictions in new stream reaches (see Appendix A3 for details). LMEM accounts for the nested data structure. As with LFEM and LFEMcf, a power variance function accounted for heteroscedasticity.

Model Validation

Correlations between RH_{\min} and Ta_{\max} —Scatterplots of RH_{\min} versus Ta_{\max} and Pearson's correlation coefficient are provided to show the relationship of RH_{\min} and Ta_{\max} within and among stream reaches in the Trask and DMS data sets.

Predictive Performance of Models—The predictive performance of the models was compared using leave-one-out cross-validation (e.g., Temesgen et al. 2008, Garber et al. 2009). One stream reach at a time was used for evaluation and the remaining $n-1$ stream reaches were used to fit the models (LFEM, LFEMcf, LMEM). The RH_{\min} values for all observations in the evaluation stream reach were predicted based on the model coefficients from the model fit of the $n-1$ stream reaches. For LFEMcf and LMEM all observations of the evaluation stream reach were used to estimate the correction factor and random stream reach effect respectively. Bias and root mean square error (RMSE) for each stream reach were calculated (see Appendix A4 for equations).

Predictive Performance by Subsample Size—To evaluate model performance by differing subsample size, a simulation study was performed, for which $n-1$ stream reaches were used to fit the models as described above. The evaluation stream reach was considered to be a new stream reach m , from which a random sample of size n_m of RH_{\min} observations were taken to estimate the correction factor and random stream reach effect to localize the model. The model performance was then evaluated based on the remaining m_i ($= n_i - n_m$) observations in stream reach m and bias and RMSE were calculated as in Equations 8 and 9 with the only difference of n_i being replaced by m_i . Subsample size n_m

ranged from 1 to 6 for the Trask and from 1 to 20 for the DMS data. The random sampling process was performed 200 times and prediction RMSE and bias were calculated for each iteration and averaged across the 200 iterations. In addition, frequency distributions of the prediction RMSE of the 200 iterations were prepared to display the change in the range and variability of prediction RMSE for LMEM and LFEMcf with increasing subsample size (Figures 4 to 7).

Results

Correlations between RH_{\min} and Ta_{\max}

RH_{\min} decreased with increasing Ta_{\max} in the DMS and Trask stream reaches (Figure 2). The DMS data exhibited larger variability within stream reaches and among stream reaches than the Trask data (Figure 2). For the Trask watershed the coefficient of correlation is $r = -0.94$ based on $n = 95$ observations across the eight stream reaches, with r values ranging from -0.39 to -0.95 within the eight stream reaches (Table 2). For the DMS data, the r values for the eight stream reaches range from -0.42 to -0.91 with an overall $r = -0.71$ for $n = 495$ across the eight stream reaches (Table 2). There was some curvature in the relationship between RH_{\min} and Ta_{\max} for the DMS stream reaches KM21 and TH46 (Figure 2).

Predictive Performance of Models

For the DMS data, including HAS and DIFN as covariates in the model in addition to Ta_{\max} decreased mean RMSE and thus improved model performance.

The predictive abilities of the three models (LFEM, LFEMcf, and LMEM) substantially differed in terms of RMSE and bias, especially for the DMS data (Table 3). For both the Trask and DMS, LFEMcf resulted in the smallest RMSE followed by LMEM. For the Trask data, the cross-validation RMSE of LFEM was 3.4% RH_{\min} . Including the correction factor (LFEMcf) or including a random stream reach effect (LMEM) decreased the RMSE by 0.6% RH_{\min} (18%) and 0.3% RH_{\min} (9%), respectively. The bias of the LFEM (-0.27%) was also decreased to 0.13% and 0.08% for LFEMcf

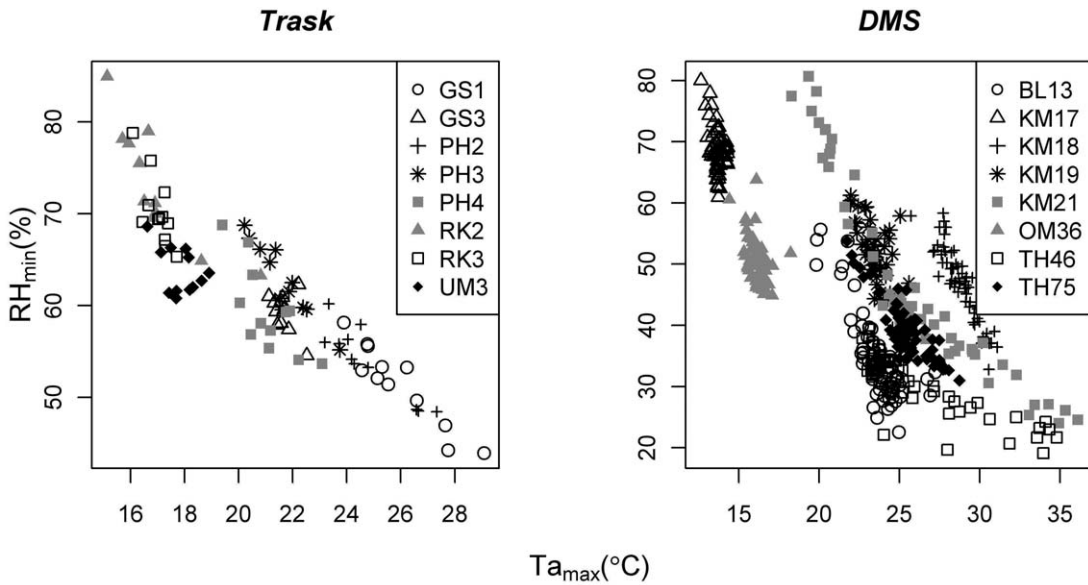


Figure 2. Mean daily minimum relative humidity (RH_{\min}) vs. mean daily maximum air (Ta_{\max}) of the eight Trask (left) and DMS (right) stream reaches. Note scale differences in x and y axes.

TABLE 2. Correlation coefficients (r) between mean daily minimum relative humidity (RH_{\min}) and mean daily maximum air temperature (Ta_{\max}) measured at approximately 1 m above ground for the n sensors available at each stream reach. 95% confidence intervals are given in parentheses.

Stream Reach	Trask		Stream Reach	DMS	
	n	r		n	r
All	95	-0.94 (-0.79, -0.94)	All	495	-0.71 (-0.66, -0.75)
GS1	12	-0.95 (-0.83, -0.99)	BL13	64	-0.80 (-0.69, -0.87)
GS3	12	-0.39 (-0.24, -0.79)	KM17	64	-0.42 (-0.19, -0.60)
PH2	12	-0.93 (-0.76, -0.98)	KM18	61	-0.86 (-0.78, -0.91)
PH3	12	-0.95 (-0.83, -0.99)	KM19	50	-0.68 (-0.50, -0.81)
PH4	12	-0.81 (-0.44, -0.94)	KM21	65	-0.91 (-0.86, -0.94)
RK2	11	-0.84 (-0.48, -0.96)	OM36	65	-0.48 (-0.27, -0.65)
RK3	12	-0.92 (-0.73, -0.98)	TH46	62	-0.86 (-0.78, -0.91)
UM3	12	-0.64 (-0.10, -0.89)	TH75	64	-0.84 (-0.75, -0.90)

TABLE 3. Cross-validation bias and root mean square error (RMSE).

Prediction method	Trask		DMS	
	RMSE (%)	Bias (%)	RMSE (%)	Bias (%)
LFEM	3.4	-0.27	10.6	-0.50
LFEMcf	2.8	-0.13	4.2	-0.04
LMEM	3.1	0.08	4.4	0.01
LMEM, fixed component	3.6	-0.48	9.7	-0.12

and LMEM, respectively (Table 3). For the DMS data, the cross-validation RMSE of LFEM was 10.60% RH_{\min} and LFEMcf and LMEM improved by 6.2% RH_{\min} (58%) and 6.4% RH_{\min} (60%), respectively. The 0.5% bias of LFEM decreased to -0.04% and 0.01% for LFEMcf and LMEM, respectively (Table 3).

If no subsample of RH_{\min} measurements is available in a new stream reach to estimate the random stream reach effect, the random effect could be set to zero and only the fixed parameters

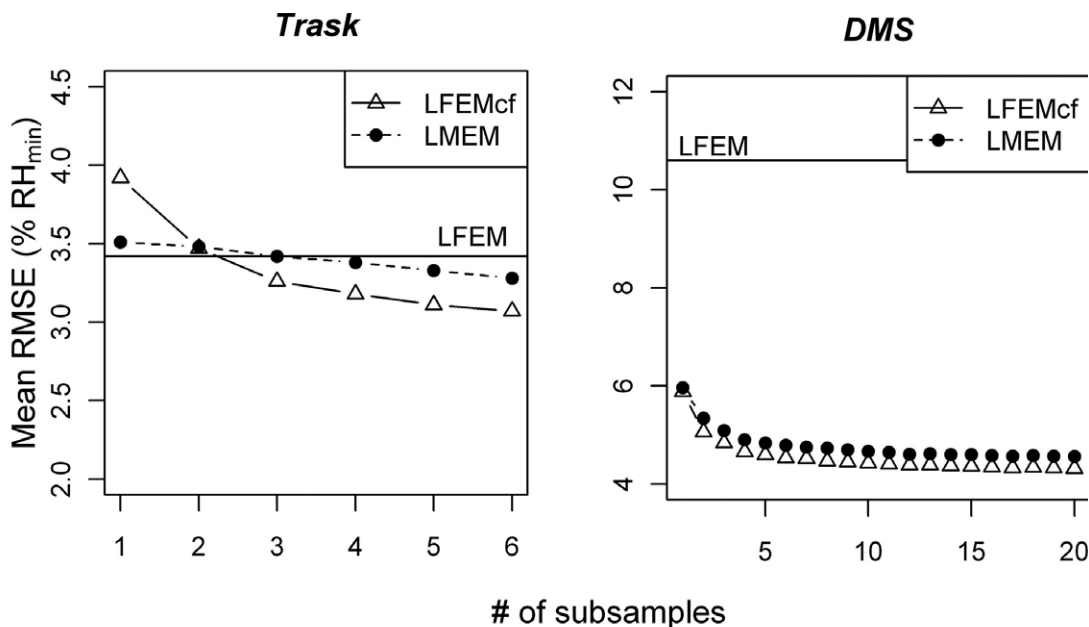


Figure 3. Predictive performance (root mean square error, RMSE) of the linear mixed effects (LMEM) and linear fixed effects model with correction factor (LFEMcf) for Trask (left) and DMS (right). Solid line: RMSE of linear fixed effects model (LFEM).

would be used for predictions. Using only the fixed parameters of the LMEM model for predictions in a new stream reach results in biased predictions and RMSE values similar to the LFEM model (Table 3, ‘LMEM, fixed component’). The LMEM fixed component model resulted in larger RMSE and bias values than LFEM for the Trask. For the DMS data, the RMSE of the LMEM fixed component model was close to the RMSE of LFEM but the bias was not quite as large as the bias for LFEM (Table 3).

Predictive Performance by Subsample Size

For the Trask, at least three subsamples of RH_{\min} were needed in a stream reach for LMEM to achieve the same or smaller prediction RMSE as LFEM. Even with more than three subsamples, the prediction RMSE only improved slightly over that of LFEM (Figure 3). Similar to LMEM three or more subsamples were needed for LFEMcf to improve prediction RMSE. The LFEMcf prediction RMSE was greater than that of LMEM for a subsample of one but smaller for subsamples

of two or more (Figure 3). Both LMEM and LFEMcf provided less biased predictions than LFEM (Table 4). With only one RH_{\min} subsample LMEM resulted in less biased predictions than LFEM, and the bias was negligible with the use of three or more subsamples to estimate the random stream reach effect. For three and more RH_{\min} subsamples LFEMcf resulted in a larger bias than LMEM (Table 4).

For the DMS data, the use of one RH_{\min} subsample for estimating the random stream reach effect and correction factor, respectively, improved the prediction RMSE and bias by almost 50% for both LMEM and LFEMcf (Figure 3, Table 4). For subsample sizes greater than 5, the improvements in prediction RMSE were negligible with further increase in subsample size (Figure 3). LFEMcf resulted in slightly smaller prediction RMSE values than LMEM when subsample sizes were greater or equal two (Figure 3). For LMEM the bias decreased with subsample sizes from one through four and was negligible when five or more subsamples were available for estimating the random stream reach effect. The bias of LFEMcf showed similar

TABLE 4. Mean bias as function of the number of RH sensors (n_m) subsampled to predict the stream reach random effect or the LFEM correction factor for the Trask (left) and DMS (right). 95% confidence intervals are given in parentheses.

n_m	Trask		DMS	
	LMEM	LFEMcf	LMEM	LFEMc
1	-0.18 (-0.23, -0.12)	-0.01 (-0.07, 0.04)	-0.26 (-0.44, -0.07)	0.27 (0.09, 0.46)
2	-0.06 (-0.12, -0.01)	-0.06 (-0.12, 0.00)	-0.28 (-0.42, -0.13)	-0.13 (-0.27, 0.02)
3	-0.04 (-0.10, 0.03)	-0.10 (-0.16, -0.04)	-0.18 (-0.31, -0.06)	-0.18 (-0.30, -0.06)
4	0 (-0.06, 0.06)	-0.11 (0.17, -0.04)	-0.10 (-0.21, 0.01)	-0.17 (-0.28, -0.06)
5	0 (-0.07, 0.07)	-0.17 (-0.24, -0.10)	-0.03 (-0.12, 0.07)	-0.09 (-0.18, 0.00)
6	0.03 (-0.04, 0.11)	-0.15 (-0.23, -0.08)	-0.02 (-0.12, 0.08)	-0.10 (-0.20, 0.00)
7			-0.03 (-0.12, 0.06)	-0.05 (-0.14, 0.04)
8			-0.03 (-0.12, 0.06)	-0.05 (-0.14, 0.04)
9			-0.02 (-0.09, 0.06)	-0.07 (-0.15, 0.00)
10			0 (-0.07, 0.07)	-0.04 (-0.12, 0.03)
15			-0.02 (-0.09, 0.04)	-0.05 (-0.12, 0.02)
20			0 (-0.06, 0.06)	-0.05 (-0.11, 0.01)

behavior but tended to be somewhat greater than the LMEM bias (Table 4).

The frequency distributions of the prediction RMSE from the 200 simulations illustrate changes in the range and variability for LMEM and LFEMcf with increasing subsample size (Figures 4 to 7). For the Trask data, the variability in prediction RMSE is smaller for LMEM for subsample sizes of $n_m = 1, 2$ and 3. The range in prediction RMSE also tends to be smaller for LMEM with the most pronounced difference for $n_m = 1$ (Figures 4 & 5). For LFEMcf with $n_m = 1$, most prediction RMSE values are greater than the cross-validation RMSE of LFEM, which changes with increase in n_m , mostly producing prediction RMSE values smaller than the cross-validation RMSE of LFEM for $n_m = 6$ (Figure 5). A similar trend is observed for LMEM (Figure 4) but not as pronounced as for LFEMcf. For the DMS data, the frequency distributions of the prediction RMSE from 200 simulations clearly narrow with increasing subsample size n_m for both LMEM (Figure 6) and LFEMcf (Figure 7). The variability and range in prediction RMSE over the 200 simulations tends to be smaller for LMEM than for LFEMcf, with the largest differences for small subsample sizes, especially $n_m = 1$ (Figures 6 and 7). For $n_m = 1$, LFEMcf produced prediction RMSE values larger than the cross-validation RMSE of LFEM.

As the subsample size n_m increases both LMEM and LFEMcf produce more RMSE values that are smaller than the cross-validation RMSE value of LMEM (Figures 6 & 7).

Discussion

Correlations between RH_{\min} and Ta_{\max}

The dry-season relationship between RH_{\min} and Ta_{\max} was more variable for the DMS than the Trask. This is attributed to the duration and timing of the microclimate sensor deployment as well as to the proximity of the stream reaches in the Trask. While RH_{\min} and Ta_{\max} averages for the Trask were based on at least four weeks of measurements and sensor deployment overlapped with three other stream reaches in a given week, the DMS averages were based on only three days without concurrent sensor deployment across reaches. The eight stream reaches in the Trask belonged to the same watershed while the DMS stream reaches were located in four different watersheds in the Oregon Coast Range. According to the observed data, the relationship between RH_{\min} and Ta_{\max} is more variable among stream reaches if daily averages are based on short sensor deployment periods because only a small snapshot in time is captured for each stream reach, which can be strongly influenced by varying weather conditions.

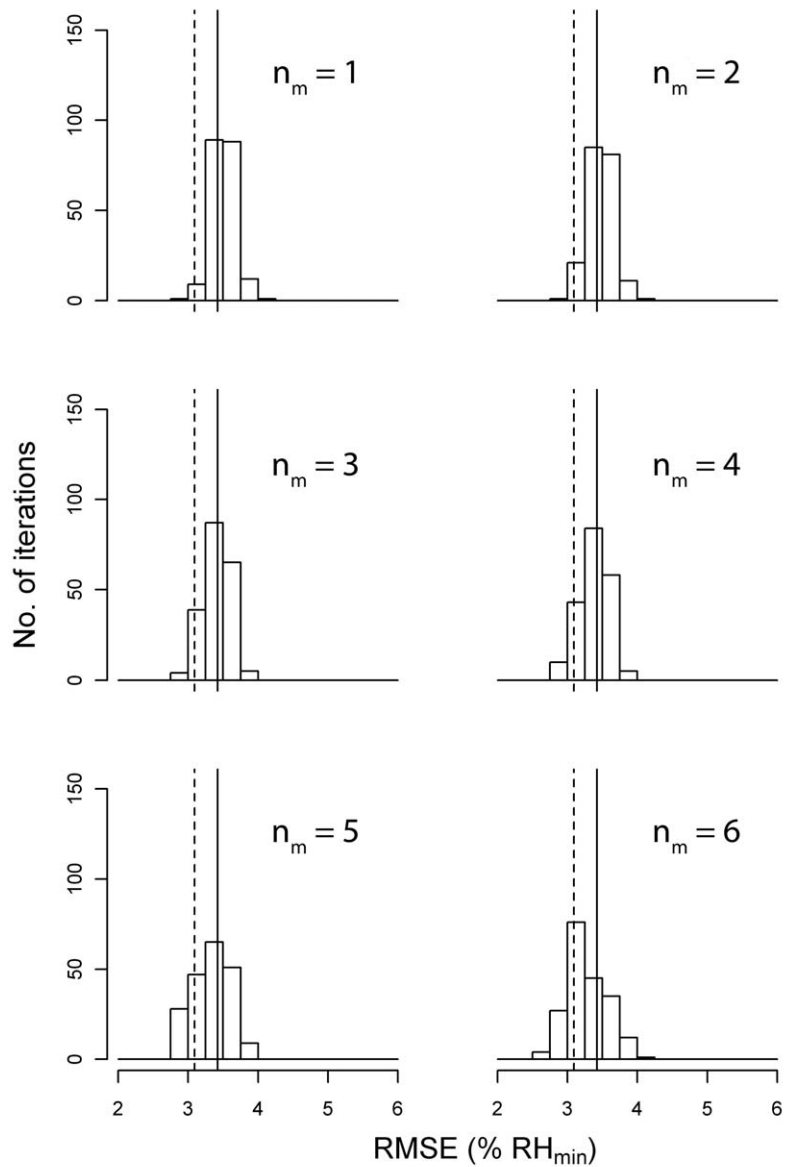


Figure 4. Frequency distribution of the root mean square error (RMSE) after 200 iterations for linear mixed effects model (LMEM) with different subsample sizes n_m for the Trask stream reaches. The cross-validation RMSE of the linear fixed effects model (LFEM; solid line) and LMEM (broken line) based on all relative humidity values are given for comparison.

The observed data also suggest that the relationship between RH_{\min} and Ta_{\max} is more variable among stream reaches if the deployment is not concurrent across stream reaches and the stream reaches cover a larger geographic range (e.g., belong to differ-

ent watersheds). If the deployment of sensors is concurrent across stream reaches within the same watershed, prevailing weather conditions result in comparable relationships between RH_{\min} and Ta_{\max} among stream reaches.

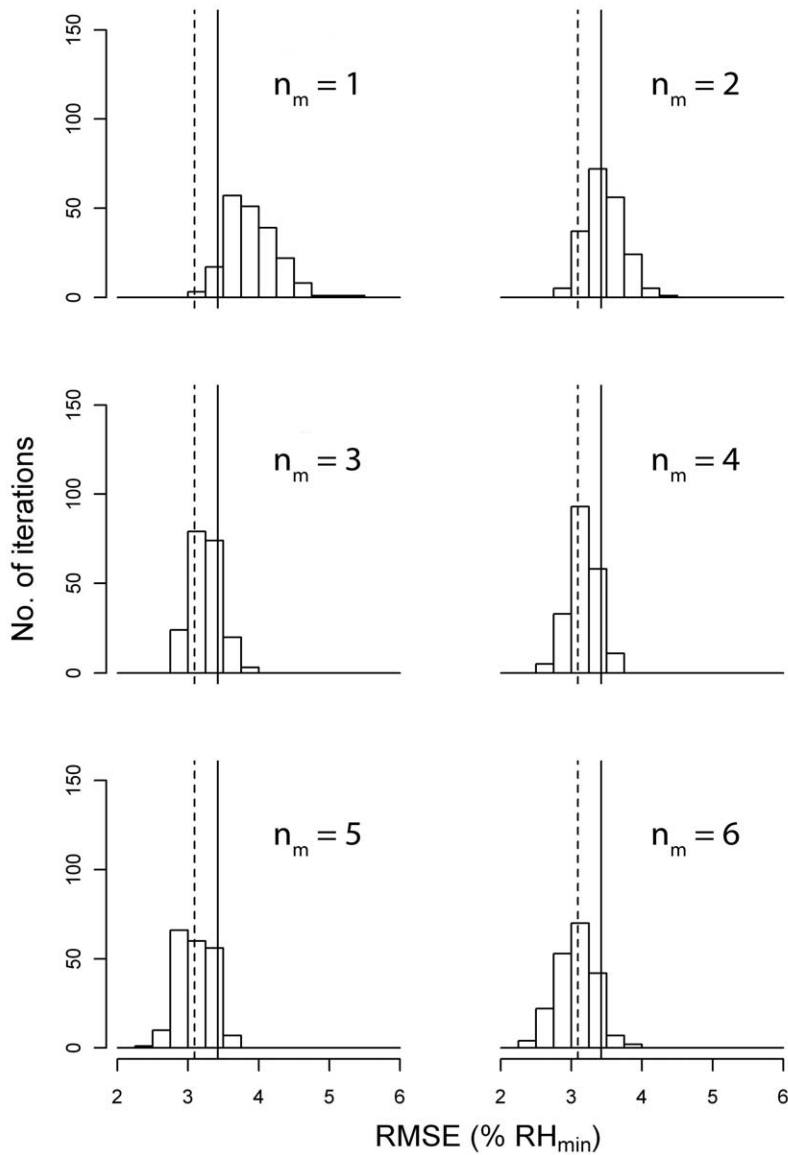


Figure 5. Frequency distribution of the root mean square error (RMSE) after 200 iterations for the linear fixed effects model with correction factor (LFEMcf) with different subsample sizes n_m for the Trask stream reaches. The cross-validation RMSE of the linear fixed effects model (LFEM; solid line) and linear mixed effects model (LMEM; broken line) based on all relative humidity values are given for comparison.

Predictive Performance of Models

The improvement of model performance for the DMS data by including DIFN and HAS as covariates suggests that variables describing shade and streamside topography are able to explain

the relative humidity gradients in riparian areas when used in combination with Ta_{\max} . In contrast, Danehy and Kirpes (2000) working east of the Cascade in more xeric systems discerned little explanatory influence of canopy cover or basal

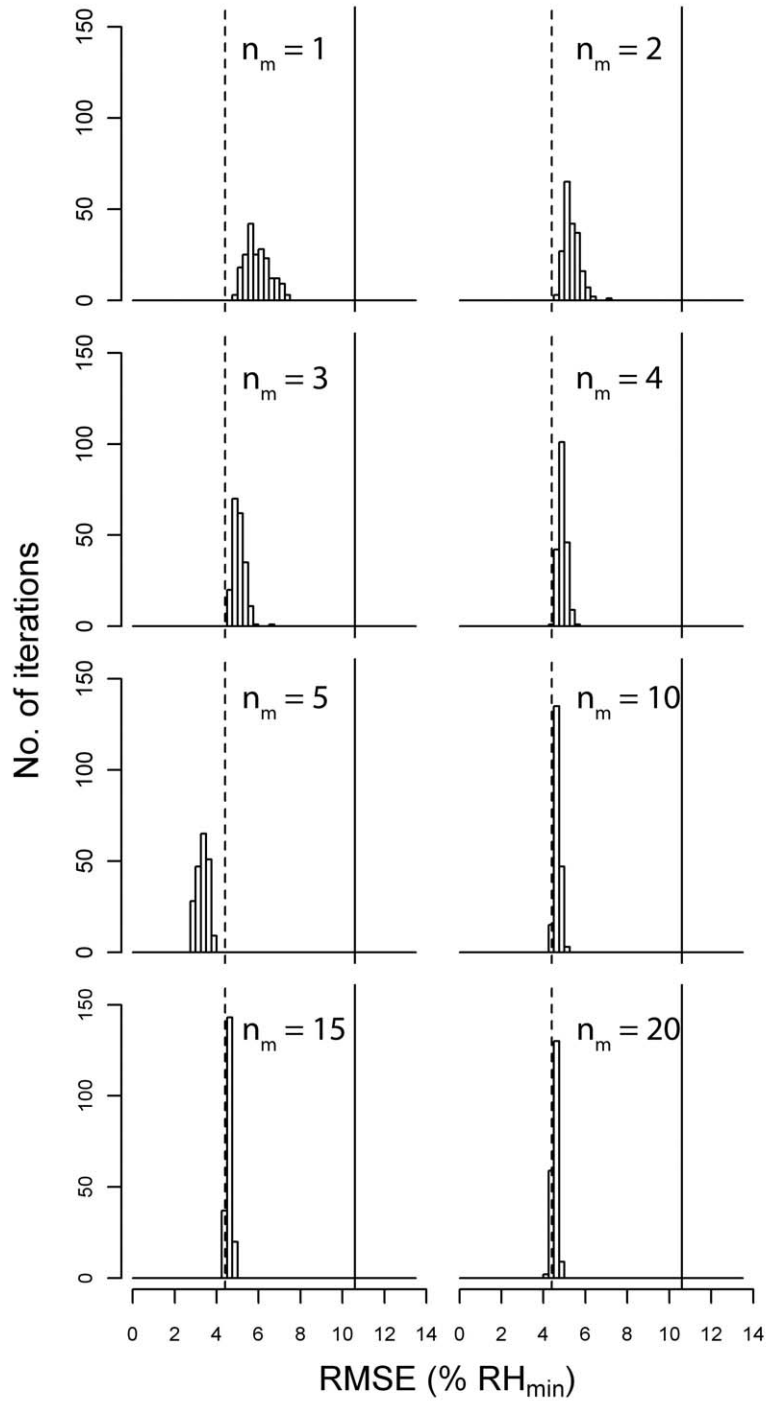


Figure 6. Frequency distribution of the root mean square error (RMSE) after 200 iterations for the linear mixed effects model (LMEM) with different subsample sizes n_m for the DMS stream reaches. The cross-validation RMSE of the linear fixed effects model (LFEM; solid line) and LMEM (broken line) based on all relative humidity values are given for comparison.

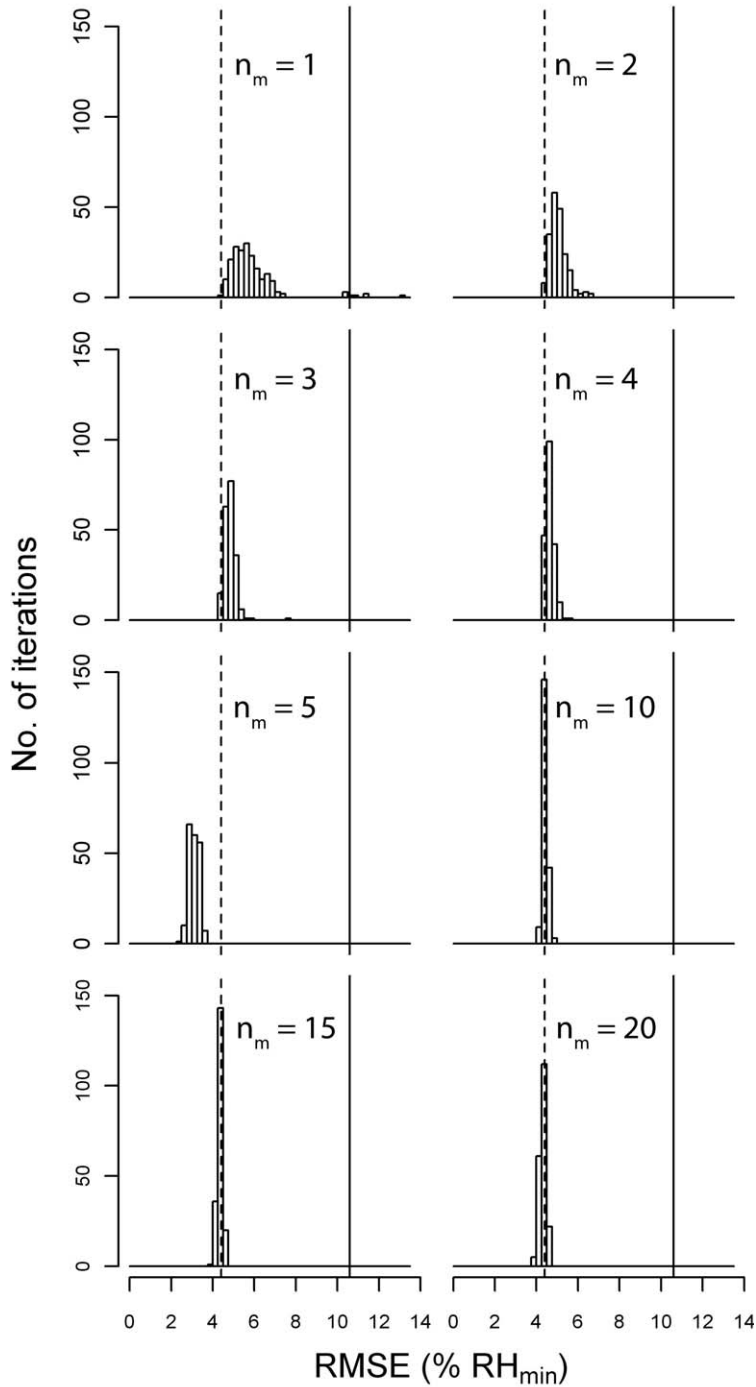


Figure 7. Frequency distribution of the root mean square error after 200 iterations for the linear fixed effects model with correction factor (LFEMcf) with different subsample sizes n_m for the DMS stream reaches. The cross-validation RMSE of the linear fixed effects model (LFEM; solid line) and the linear mixed effects model (LMEM; broken line) based on all relative humidity values are given for comparison.

area in regression models describing gradients of relative humidity. They attributed this lack of influence on the highly variable, patchy distribution of both understory shrubs and overstory trees in the pine-dominated forests. Our findings indicate that covariates that describe changes in overstory cover or other streamside stand structure attributes may indeed be used to model the impact of management activities on RH_{\min} in riparian areas west of the Cascades if Ta_{\max} information is available.

Covariates such as channel orientation (aspect), elevation, topography (e.g., influences of steep valley confinement), and the occurrence of rain are expected to influence RH and Ta_{\max} . Because these are covariates at the stream reach level, their impact should be captured by the random stream reach effect of the models. Hence, none of these covariates were included in the models.

Substantial differences were found among the predictive abilities of the alternative strategies examined for developing RH equations. LFEMcf and LMEM outperformed LFEM in terms of accuracy and precision because LFEM ignores the nested data structure and assumes that all RH_{\min} measurements are independent, whereas LFEMcf and LMEM account for the nested data structure and allow localization of the RH_{\min} model for each stream reach. RMSE and bias of LFEM were greater for the DMS than the Trask because the DMS data exhibited greater variability among stream reaches than the Trask data. Hence, accounting for the nested data structure by using a correction factor (LFEMcf) or including a random stream reach effect (LMEM) resulted in greater improvement in terms of accuracy and precision for the more variable DMS data.

LFEM had substantial bias for both the Trask and DMS data. Therefore, LFEM should not be used for modeling RH_{\min} across stream reaches since it ignores the nested data structure. The RH_{\min} model should be localized for each stream reach with subsampled information using LFEMcf or LMEM. Even though LFEMcf resulted in slightly smaller RMSE values than the LMEM for both the Trask and DMS data, the less biased LMEM is superior to the LFEMcf, which can still be biased,

even though the bias is smaller in comparison to that observed for LFEM without correction factor.

It is surprising that LMEM performed slightly worse in terms of RMSE than LFEMcf. Temesgen et al. (2008) applied nonlinear models to predict tree heights that were localized with subsampled tree heights. In their study the fixed effects model with correction factor performed worse than the mixed effects model. It is possible that the DMS and Trask data did not have enough stream reaches (8 each) as well as not enough observations within a stream reach available (12 for Trask, 50 to 65 for DMS) to reliably estimate the variance components in the mixed effects model framework. As found in previous studies (Monleon 2003, Temesgen et al. 2008), it is not recommended to use only the fixed components of a mixed effects model, if no subsamples are available, since this can produce worse predictions in terms of RMSE and bias than using a fixed effects model that ignores the nested data structure completely.

Predictive Performance by Subsample Size

Localizing the model with only one RH_{\min} subsample improved the model performance substantially for the DMS data that exhibited larger variability among stream reaches. For the Trask data, which exhibited less variability among stream reaches, the model improvement was much smaller even when several subsamples were used for localization of the model. Localizing the model based on only one or two subsamples can even decrease model performance in comparison to a fixed effects model that ignores the nested data structure if the data set exhibits little variability among stream reaches. Based on the results of our study, a minimum of three to five subsamples are needed to estimate the random stream reach effect or the stream reach correction factor, and that the model improvements will be greater when the variability among stream reaches is high.

The range and variability of prediction RMSE of LFEMcf tended to be larger than for LMEM. This was most pronounced for small subsample sizes. In addition, LFEMcf tended to result in larger bias than LMEM. This suggests that the LMEM

approach is superior to the LFEMcf, especially for small subsample sizes of one or two.

Although microclimate sampling and monitoring costs are predominately driven by time and expenses associated with travel, the cost of equipment (microclimate sensors) can be decreased by only subsampling for relative humidity. If sensors that measure both relative humidity and temperature are four times more expensive than sensors that measure temperature only, the equipment cost can be cut in half by subsampling relative humidity at one third of all the locations for which temperature information is recorded.

Our analysis does not support recommendations on where to place the subsample of RH sensors. However, the sensors should be placed so that they capture the full range of RH values within a stream reach (e.g., close to stream and on ridge top). Deploying air temperature sensors densely along fewer transects was found to be more efficient for modeling purposes than widely spaced deployment along a larger number of transects (Eskelson et al. 2011). The same may be true for RH sensor deployment.

Accuracy and Applicability

The importance of atmospheric humidity to defining the fundamental niche and activity levels of riparian forest organisms, particularly amphibians and macroinvertebrates, is well established (e.g., Dumas 1956, Feder 1983, Collier and Smith 2000); however, critical thresholds of relative humidity are lacking. The RMSE of the models developed here indicate prediction errors of 3-4% relative humidity. This level of precision is likely suitable for distinguishing among somewhat broadly defined humidity regimes arising from different stream reach conditions (e.g., degree of channel incision, seasonal presence of surface water, stream orientation, geographic location). The extent to which estimation precision is relevant to detecting relative humidity responses to forest management—particularly harvest—will likely be strongly dependent on the intensity of perturbation. Overstory removal (clear cutting) has been associated with decreased relative humidity of 10-15% when expressed as a daily average (Chen

et al. 1993, Brosofske et al. 1997), or as much as 20-30% when expressed as the summer mean daily minimum (Chen et al. 1995, Rykken et al. 2007). In contrast to complete overstory removal, partial overstory removal (thinning) has been associated with relative humidity decreases of typically less than 10% and in many cases negligible (Anderson et al. 2007, Brooks and Kyker-Snowman 2008). When the question becomes one of degree of relative humidity response with a small incremental change in harvest intensity, it is unlikely that the prediction error of the presented models will be sufficiently small to accurately predict small changes in relative humidity. The minimum effect size for accurate detection has yet to be determined and will likely vary substantially with site conditions.

Another complexity arises from the inherent capabilities (design limitations) of various sensors to accurately measure the target environmental parameters. The relative humidity sensors commonly used in ecological field studies have an accuracy of $\pm 2-3\%$. In contrast, the sensors commonly deployed for temperature measurement have accuracies typically in the range of $\pm 0.5\text{ }^{\circ}\text{C}$. Sensor errors arise from variability in the physical responses of sensor components to the environment and the inability of a modeled calibration function to fully account for this inconsistency (Wobker et al. 2010). Thus the modeling of relative humidity based on temperature data will have an inherent limit of 2-3% resolution due to measurement error. This level of measurement error is not reflected in the RMSE calculated for the fitted models, which assumes that both the explanatory and dependent variables are measured without error. While model precision of estimation can be improved by increasing the number of independent data points, the measurement error associated with limitations of the sensor calibration function cannot be decreased by simply making more measurements or deploying more sensors (sensu Gregoire et al. 1995, Wobker et al. 2010). The RMSE of the RH_{\min} estimation models fitted here suggests their utility for modeling RH_{\min} patterns in a general context but perhaps not for high resolution individual point estimation. In our modeling we used daily averages as integrative metrics of relative humidity and air temperature.

Assuming that sensor measurement error is unbiased, models developed from integrative metrics may be less susceptible to measurement error and therefore may have more predictive utility than models developed from individual observations, but we did not explicitly address this possibility. The inherent measurement error of relative humidity due to sensor design limitations could be accounted for in future models by following Carroll et al. (2006:239-245).

Although forest managers have substantial interest in monitoring temperature responses to harvest, particularly in relation to the influences of an altered microclimate on critical stream temperature thresholds, there has been substantially less interest or experience in monitoring relative humidity changes due to management activity. Within a holistic ecosystem management paradigm the recognition that atmospheric humidity as well as temperature may have importance in defining habitat suitability for some organisms or communities, there may be value to defining cost-efficient ways to monitor relative humidity patterns and dynamics. For example, the assessment of novel silvicultural approaches to restore riparian processes and functions might consider relative humidity as an element of a broader suite of forest structure and microclimate attributes to monitor. The modeling approaches presented here provide one means for enhancing relative humidity effectiveness monitoring predominantly in a research context but potentially in adaptive management applications as well.

Future Research

A few stream reaches in the DMS data showed some curvature in the relationship between RH_{\min} and Ta_{\max} . This may be accommodated in the models by adding quadratic terms. The slope in the relationship between RH_{\min} and Ta_{\max} differed slightly for some of the DMS stream reaches. This could possibly be accounted for by adding a random slope in the linear mixed effects model. Due to the fairly small data sets used in our study, neither the random slope nor the quadratic terms were explored any further because they would have required the estimation of additional parameters.

However, these are possible ways to improve the presented models in the future as more data become available. Future models should also explore the inclusion of variables that describe canopy cover and shade in more detail, which may allow additional assessment of management activity impacts on relative humidity in riparian areas.

In our study, data measured in a single summer were used for the model development. To cut back on RH_{\min} monitoring costs, it is mainly of interest to make use of RH_{\min} measurements from previous years. Based on the results of our study, incorporating RH_{\min} information from previous years into the RH_{\min} models will improve model accuracy.

It may also be beneficial to extend the modeling effort beyond the warm, dry summer season, which has been the focus of stream-centric water temperature and microclimate studies to address seasonal variation in the relationships between microclimate and distance from stream. Microclimate-distance from stream relationships have been shown to vary across seasons not only with respect to horizontal distance from stream (Hannah et al. 2008), but also with respect to vertical distance in the canopy (Rambo and North 2008). Conceivably, seasonal variation in horizontal and vertical gradients could play important roles in the structuring of habitats during important life history stages for many organisms (McCune 1993, Pabst and Spies 1998, Sheridan and Olson 2003) in addition to posing complex modeling challenges.

Conclusions

High relative humidity levels in riparian areas are paramount for riparian flora and fauna. It is practically impossible to monitor relative humidity for all stream reaches that are potentially impacted by forest management activities. We presented relative humidity models that may allow a cost-effective way of monitoring riparian relative humidity and localizing relative humidity information to specific stream reaches to inform buffer prescriptions. The presented LMEM and LFEMcf models allowed predictions of RH_{\min} based on Ta_{\max} and other covariates by localizing the model for new stream reaches with an estimated random stream reach effect or stream reach correction factor, respec-

tively. Based on our results, a minimum of three to five RH_{\min} subsamples per stream reach are recommended for estimating the random effect or correction factor, but substantial improvements in model performance can already be achieved with a subsample size of one if the variability among stream reaches is large. Model improvement was greater for the DMS data compared to the Trask, which had less variability among stream reaches than was observed in the DMS data. Subsampling of relative humidity can potentially reduce equipment costs for microclimate monitoring. However, it is still uncertain whether the prediction accuracy achieved by our presented models is sufficient for detecting change in relative humidity caused by management activities. Future RH_{\min} models

could possibly be improved by incorporating RH_{\min} measurements from previous years and accounting for the response error.

Acknowledgements

This research was funded in part by the USDA Forest Service, Pacific Northwest Research Station, and the USDI, Bureau of Land Management, Oregon State Office, agreement HA-I01-0010. The microclimate data collection in the Trask watershed was funded by the USGS Forest and Rangeland Ecosystem Science Center. We thank the editor and reviewers of Northwest Science for their valuable comments and feedback throughout the review process.

Literature Cited

- Anderson, P. D., D. J. Larson, and S. S. Chan. 2007. Riparian buffer and density management influences on microclimate of young headwater forests of western Oregon. *Forest Science* 53:254-269.
- Brooks, R. T., and T. D. Kyker-Snowman. 2008. Forest floor temperature and relative humidity following timber harvesting in southern New England, USA. *Forest Ecology and Management* 254:65-73.
- Brooks, R. T., and T. D. Kyker-Snowman. 2009. Forest-floor temperatures and soil moisture across riparian zones on first- to third-order headwater streams in southern New England, USA. *Forest Ecology and Management* 258:2117-2126.
- Broszofske, K. D., J. Chen, R. J. Naiman, and J. F. Franklin. 1997. Harvesting effects on microclimatic gradients from small streams to uplands in western Washington. *Ecological Applications* 7:1188-1200.
- Carroll, R. J., D. Ruppert, L. A. Stefanski, and C. M. Crainiceanu. 2006. *Measurement Error in Nonlinear Models. A Modern Perspective*, 2nd ed. Chapman & Hall/CRC, Boca Raton.
- Chen, J., J. F. Franklin, and T. A. Spies. 1993. Contrasting microclimates among clearcut, edge, and interior of old-growth Douglas-fir forest. *Agricultural and Forest Meteorology* 63:219-237.
- Chen, J., J. F. Franklin, and T. A. Spies. 1995. Growing-season microclimatic gradients from clearcut edges into old-growth Douglas-fir forests. *Ecological Applications* 5:74-86.
- Chen, J., S. C. Saunders, T. R. Crow, R. J. Naiman, K. D. Broszofske, G. D. Mroz, B. L. Brookshire, and J. F. Franklin. 1999. Microclimate in forest ecosystem and landscape ecology: Variations in local climate can be used to monitor and compare the effects of different management regimes. *BioScience* 49:288-297.
- Cissel, J. H., P. D. Anderson, D. Olson, K. P. Puettmann, S. Berryman, S. S. Chan, and C. Thompson. 2006. BLM density management and riparian buffer study: establishment report and study plan. U.S. Geological Survey, Scientific Investigations Report 2006-5087.
- Collier, K. J., and B. J. Smith. 2000. Interactions of adult stoneflies (Plecoptera) with riparian zones I. Effects of air temperature and humidity on longevity. *Aquatic Insects* 22:275-284.
- Danehy, R. J., and B. J. Kirpes. 2000. Relative humidity gradients across riparian areas in eastern Oregon and Washington forests. *Northwest Science* 74:224-232.
- Dumas, P. C. 1956. The ecological relations of sympatry in *Plethodon dunni* and *Plethodon vehiculum*. *Ecology* 37:484-495.
- Eskelson, B. N. I., P. D. Anderson, H. Temesgen, and J. C. Hagar. 2011. Geostatistical modeling of riparian forest microclimate and its implications for sampling. *Canadian Journal of Forest Research* 41:974-985.
- Feder, M. E. 1983. Integrating the ecology and physiology of plethodontid salamanders. *Herpetologica* 39:291-310.
- Garber, S.M., Temesgen, H., V.J. Monleon, and D.W. Hann. 2009. Effects of height imputation strategies on stand volume estimation. *Canadian Journal of Forest Research* 39:694-703.
- Gomi, T., R. C. Sidle, and J. S. Richardson. 2002. Understanding processes and downstream linkages of headwater streams. *BioScience* 52:905-915.
- Gregoire, T. G., H. T. Valentine, and G. M. Furnival. 1995. Sampling methods to estimate foliage and other characteristics of individual trees. *Ecology* 74:1181-1194.
- Hannah, D. M., I. A. Malcolm, C. Soulsby, and A. F. Youngson. 2008. A comparison of forest and moorland

- stream microclimate, heat exchanges and thermal dynamics. *Hydrological Processes* 22:919-940.
- Jones, H. G. 1992. *Plants and Microclimate: A Quantitative Approach to Environmental Plant Physiology*. 2nd Ed. Cambridge University Press, Cambridge, UK.
- Landsberg, J. J. 1986. *Physiological Ecology of Forest Production*. Academic Press, London, UK.
- McCune, B. 1993. Gradients in epiphyte biomass in three *Pseudotsuga-Tsuga* forests of different ages in western Oregon and Washington. *Bryologist* 96:405-411.
- Monleon, V. J. 2003. A hierarchical linear model for tree height prediction. *In: Proceedings of the 2003 Meeting of the American Statistical Association*. Section on Statistics and the Environment, 3-7 August 2003, San Francisco, California. The American Statistical Association, Alexandria, Virginia. Pp. 2865-2869.
- Nakano, S., and M. Murakami. 2001. Reciprocal subsidies: dynamic interdependence between terrestrial and aquatic food webs. *Proceedings of the National Academy of Sciences of the United States of America* 98:166-170.
- Olson, D. H., P. D. Anderson, M. P. Hayes, C. A. Frissell, and D. F. Bradford. 2007. Biodiversity management approaches for stream riparian areas: perspectives for Pacific Northwest headwater forests and amphibians. *Forest Ecology and Management* 246:81-107.
- Olson, D. H., and G. Weaver. 2007. Vertebrate assemblages associated with headwater hydrology in western Oregon managed forests. *Forest Science* 53:343-355.
- Pabst, R. J., and T. A. Spies. 1998. Distribution of herbs and shrubs in relation to landform and canopy cover in riparian forests of coastal Oregon. *Canadian Journal of Botany* 76:298-315.
- Pinheiro, J. C., and D. M. Bates. 2000. *Mixed-effects Models in S and S-plus*. Springer, New York.
- R Development Core Team. 2011. *R: A language and environment for statistical computing*. R Foundation for Statistical Computing, Vienna, Austria. ISBN 3-900051-07-0. Available online at: <http://www.R-project.org/> (accessed 15 July 2011).
- Rambo, T. R., and M. P. North. 2008. Spatial and temporal variability of canopy microclimate in a Sierra Nevada riparian forest. *Northwest Science* 82:259-268.
- Rykken, J. J., S. S. Chan, A. R. Moldenke. 2007. Headwater riparian microclimate patterns under alternative forest management treatments. *Forest Science* 53:270-280.
- Sheridan, C.D., and D. H. Olson. 2003. Amphibian assemblages in zero-order basins in the Oregon Coast Range. *Canadian Journal of Forest Research* 33:452-1477.
- Sheridan, C. D., and T. A. Spies. 2005. Vegetation-environment relationships in zero-order basins in coastal Oregon. *Canadian Journal of Forest Research* 35:340-355.
- Temesgen, H., V. J. Monleon, and D. W. Hann. 2008. Analysis and comparison of nonlinear tree height prediction strategies for Douglas-fir forests. *Canadian Journal of Forest Research* 38:553-565.
- Trask Study Plan. 2008. Effects of contemporary forest harvest on aquatic ecosystems: Trask river watershed study. Available online at: <http://watershed-sresearch.org/Trask/StudyDesign.html> (accessed 30 November 2011).
- Wobker, M. E. S., A. Mehrotra, and B. H. Carter. 2010. Use of commercial data loggers to develop process understanding in pharmaceutical unit operations. *Journal of Pharmaceutical Innovation* 5:169-180.

Received 22 March 2012

Accepted for publication 12 October 2012

Appendix

A1. Linear Fixed Effects Model

The linear fixed effects model is specified as:

$$[1] \quad RH_{\min ij} = \mathbf{X}_{ij}\boldsymbol{\beta} + \varepsilon_{ij}$$

where $RH_{\min ij}$ is the mean daily minimum relative humidity measured for sensor j in stream reach i ; \mathbf{X}_{ij} are the covariates observed for sensor j in stream reach i (i.e., $Ta_{\max ij}$ for the Trask and $Ta_{\max ij}$, HAS_{ij} , and $DIFN_{ij}$ for DMS); $\boldsymbol{\beta}$ are parameters to be estimated; and ε_{ij} is an error term, assumed to be independent between observations and with $N(0, \sigma_\varepsilon^2 Ta_{\max ij}^{2\delta})$ where the parameter δ can take any value in the real line. The variance structure of the within-stream reach errors was modeled with a power variance function (Pineiro and Bates 2000, p. 210). To predict RH values for locations in a new stream reach m the available information of the covariates $Ta_{\max ij}$, HAS, and DIFN is simply applied to Equation 1:

$$[2] \quad \hat{RH}_{\min m, new} = \mathbf{X}_{m, new}\hat{\boldsymbol{\beta}}$$

where $\mathbf{X}_{m, new}$ are the covariates at the new locations in stream reach m and $\hat{\boldsymbol{\beta}}$ are the parameter estimates from Equation 1.

A2. Linear Fixed Effects Model with Correction Factor

The correction factor k_m^* for the LFEMcf model is calculated as:

$$[3] \quad k_m^* = \frac{\sum_{j=1}^{n_m} \left(\frac{\hat{RH}_{\min mj} RH_{\min mj}}{Ta_{\max mj}^{2\delta}} \right)}{\sum_{j=1}^{n_m} \left(\frac{\hat{RH}_{\min mj}^2}{Ta_{\max mj}^{2\delta}} \right)}$$

where $\hat{RH}_{\min mj}$ and $RH_{\min mj}$ are the predicted and observed RH_{\min} values for the sensor j in the

new stream reach m . The localized prediction for a new location in stream reach m is then:

$$[4] \quad \hat{RH}_{\min m, new} = k_m^* * \mathbf{X}_{m, new}\hat{\boldsymbol{\beta}}$$

where $\mathbf{X}_{m, new}$ and $\hat{\boldsymbol{\beta}}$ are defined as in Equation 2 and k_m^* is the stream reach correction factor.

A3. Linear Mixed Effects Model

The linear mixed effects model is defined as follows:

$$[5] \quad RH_{\min ij} = \mathbf{X}_{ij}\boldsymbol{\beta} + b_i + \varepsilon_{ij}$$

where \mathbf{X}_{ij} and $\boldsymbol{\beta}$ are defined as in Equation 1, and $b_i \sim N(0, \sigma_b^2)$ and $\varepsilon \sim N(\mathbf{0}, \sigma_\varepsilon^2 \boldsymbol{\Sigma})$ are the random stream reach effect and residual error term, respectively, with $\boldsymbol{\Sigma}$ being a diagonal matrix with elements $Ta_{\max ij}^2$. The variance structure of the within-stream reach errors was modeled with a power variance function (Pineiro and Bates 2000, p. 210).

If a subsample n_m of RH_{\min} measurements is available from a new stream reach m not included in the original modeling data set, the subsample can be used to localize RH_{\min} predictions for that stream reach using the parameter estimates obtained by fitting Equation 5:

$$[6] \quad \hat{RH}_{\min m, new} = \mathbf{X}_{m, new}\hat{\boldsymbol{\beta}} + \hat{b}_m$$

where \hat{b}_m is the estimated random stream reach effect for new stream reach m . For a particular stream reach for which a subsample of RH_{\min} measurements is available \hat{b}_m is estimated as

$$[7] \quad \hat{b}_m = \hat{\sigma}_b^2 \mathbf{1}_{n_m}' (\hat{\sigma}_b^2 \mathbf{J}_{n_m} + \hat{\sigma}_\varepsilon^2 \boldsymbol{\Sigma})^{-1} (\mathbf{RH}_{\min m} - \mathbf{X}_m \hat{\boldsymbol{\beta}})$$

where $\mathbf{1}_{n_m}'$ is a vector of ones with length n_m , \mathbf{J}_{n_m} is a $n_m \times n_m$ matrix of ones, and $\mathbf{RH}_{\min m}$ and $\mathbf{X}_m \hat{\boldsymbol{\beta}}$ are the observed and predicted RH_{\min} values of the subsample in stream reach m .

A4. Bias and Root Mean Square Error

Bias and root mean square error (RMSE) for each stream reach were calculated as follows:

$$[8] \text{ Bias} = \frac{1}{n} \sum_{i=1}^n \left[\frac{1}{n_i} \sum_{j=1}^{n_i} \left(RH_{\min ij} - \hat{RH}_{\min ij} \right) \right]$$

$$[9] \text{ RMSE} = \frac{1}{n} \sum_{i=1}^n \sqrt{\frac{1}{n_i} \sum_{j=1}^{n_i} \left(RH_{\min ij} - \hat{RH}_{\min ij} \right)^2}$$

where n is the number of stream reaches, n_i is the number of deployed microclimate sensors within stream reach i , and $\hat{RH}_{\min ij}$ and $RH_{\min ij}$ are the predicted and observed RH_{\min} values for the sensor j in stream reach i , respectively. The average bias and RMSE of the eight stream reaches was reported.